Procedia
Environmental Science,
Engineering and Management
http://www.procedia-esem.eu

Procedia Environmental Science, Engineering and Management, **4** (2017) (4) 207-218

International Symposium on Soil and Water Bioengineering in a Changing Climate,
7th-8th September, 2017, Glasgow, Scotland, UK

ON THE TREE STABILITY: PULLING TESTS AND MODELLING TO ASSESS THE ROOT ANCHORAGE*

Yamuna Giambastiani[1], Federico Preti[1], Alessandro Errico[1], Luigi Sani[2]**

[1]GESAAF Department of Agricultural, Food and Forestry Systems – University of Florence
[2]GIFOR per gli alberi – Florence

Abstract

In addition to increasing temperatures and exacerbating meteorological extreme events, climate change affects the frequency of windstorms, which impact the stability of trees in urban and periurban environments. Therefore, there is growing interest in developing models for predicting how root anchorage could influence tree stability. Root anchorage depends on roots morphology and architecture and their relative interaction with soil. The present study aims to assess the safety factor (SF) of trees through a simple static model considering overturning moment and anchorage strength. 21 trees, in 5 sites located in 5 sites in Tuscany (North-Western Italy), were subjected to pulling tests simulating the wind force. Pulling tests were executed following similar works. The applied load was assessed in relation with the RAR (Root Area Ratio) measured for each tree. Through the model is able to calculate the root plate radius (Rt). The results show that the low-load pulling test is effective in predicting the tree overturning load, and that tree stability is influenced by the equilibrium between the roots distribution and the lateral space to grow. Rt varied in the range of 4-12 times the stem radius and this multiplication factor resulted linked with mean rooting depth. This approach could be used for slope stability analysis when considering also the effects of root cohesion.

Key words: biomechanics, root morphology, RAR, tree overturning, wind loading

* Selection and peer-review under responsibility of the ECOMED project consortium
** Corresponding author: e-mail: yamuna.giambastiani@unifi.it

1. Introduction

The main cause of tree failure is represented by the wind load (Coutts et al., 1995). In literature, various studies were conducted concerning tree stability with a biomechanical approach, in static or in dynamic conditions. Peltola et al. (2006) assessed the maximum bending moment (BMmax) for tree failure by pulling tests, working in static conditions. BMmax was also studied for different soil types (Moore, 2000) and different species (Peltola et al., 2000). Other studies were carried out under dynamic load, measuring the tilt of the root plate, by means of high frequency accelerometers installed on plants subjected to natural wind load (James et al., 2013; Schindler, 2008). Different studies concern the root anchorage under wind load (Coutts, 1983; Danjon et al., 2005) and the influence of root morphology (Fourcaud et al., 2008; Mickovski et al. 2007). Their findings demonstrated that the root system grows adapting to the stresses, by which it is subjected (Lundström et al., 2007). In addition to the overturning, another mechanism of tree failure is the stem breakage (Skatter et al., 2000). This phenomenon depends, among other factors, on tree age and uncustomary wind direction (Stokes, 1999).

The existing models employ dimensional parameters of plants such as DBH, Height, tree weight, etc., in relation to wind load (Cucchi et al., 2005; Schelhaas et al., 2007) or BMmax (Mattheck et al., 2000). The models are constructed by field analysis or wind tunnel experiments (Gardiner et al., 1993). Some models also introduce hypogea parameters such as CSA (Cross-sectional area), root plate radius (Rahardjo et al., 2014) and root architecture (Dupuy et al., 2005). Additional studies were also presented on the plant response subjected to wind action with a botanical approach, focusing on physiological mechanisms such as mechanoperception (Telewsky, 2006) and thigmomorphogenesis (Pruyn et al., 2000). In addition, based on the constant stress axiom (Mattheck et al., 1997), tree stability is assessed in terms of plant's ability to adapt, through the mechanosensitive control of growth (Moulia et al., 2015). With this study, the authors do notnot seek to assess the stability of investigated trees, in relation to wind load. Wind forces are dynamic and extremely variable, both spatially and temporally (James et al. 2008). A static approach is not able to reproduce the induced stresses (due to twisting, turbulence, rapid direction change), which interfere with crown architecture (Rudnicki et al., 2001). This considered, the aim of the present paper is to assess tree stability introducing a simple numerical model that links an exterior load with root anchorage in terms of root cohesion. The presented method was derived from the well-known methods of vegetated slope stability assessment (Greenwood, 2006), where the contribution of roots represents often a key-factor in determining the soil cohesion, and therefore its shear stress resistance. A common parameter used to express the root density within a soil is the Root Area Ratio (*RAR*), which is a main parameter to assess the root cohesion (CV), contributing to the total soil cohesion. *RAR* represents the ratio between the area of roots and the total area of a soil section. *RAR* follows a negative exponential law depending on the rooting depth Eq. (1):

$$RAR(z) = RAR_0 \, e^{-z/b} \tag{1}$$

where: z is the depth (m), RAR_0 (-) represents the scale factor, closely correlated to the DBH (diameter at breast height), b is defined as the mean rooting depth (m). The factor "b" can be measured on field, with destructive methods, digging a vertical profile close to the plant, or it can be estimated using an ecohydrological model, function of the site characteristics, such as Preti et al. (2010) or Tardìo et al. (2016). The proposed model calculates SF (safety factor) as the ratio between the stabilizing and destabilizing moments.

RAR parameter is needed to calculate the stabilizing moment for the cohesion between the soil and the root plate.

2. Materials and method

2.1. Trees and sites

The trees used in this study were object of urban re-planning, thus destined for felling. During the analysis, the trees were subjected to strong mechanical stresses and root system alterations. Hence, to ensure the safety of the experimental site, it was necessary to remove the plants after the test. Trees removal was not due because of phytostatic or phytosanitary purposes, but for the reorganization of the urban site. In fact, the plants were in good vegetative conditions and did not show significant defects that could compromise stability. Tests were carried out on 21 trees in 5 sites in Tuscany (Fig. 1).

Fig. 1. Geographic position of the cases of study

Specifically: 4 trees of the specie *Pinus pinea* (Stone pine) in San Rossore (PI), 4 Stone pines in Arezzo, 1 *Alnus glutinosa* (Alder) in Pomezzana (LU), 1 *Populus nigra* (Poplar) in Virginio (FI), 1 *Fraxinus angustifolia* (Ash) and 10 *Picea abies* (Spruce) in Quaracchi (FI) (Fig. 2). All these species are endemic in Italy and are representative of stands that suffer wind-throw in forests and cause damages in urban environment. For each tree, we recorded height, DBH and crown area. Volume was estimated by two-way table (IFCN - Tabacchi et al., (2011)), while weight was calculated by the volume, through green wood density (IPCC, 2003) (Table.1).

Table 1. Stationary features and soil parameters of study cases – f (°) is angle of friction, Sw is degreed to saturation

Site	*Prov*	*Location*	*Coordinates*	*Altitude*	*Soil*	*φ(º)*	S_w
Arezzo	AR	Urban	43º28’16.9” N	296 m asl	Anthropogenic	25	0.3
Pomezzana	LU	Apuan Alps	43º59’14.5” N	605 m asl	Silty clay loam	32	0.4
Quaracchi	FI	Urban	43º47’40.6” N	44 m asl	Anthropogenic	32	0.3
San Ressore	PI	Coast	43º44’03.6” N	1 m asl	Sand	22	0.2
Virginio	FI	Riparian	43º37’54.7” N	143 m asl	Sediment	20	0.6

Data were collected in January-March 2017, during period of vegetative rest. All sites have a Mediterranean climate of hot dry summers and cool moist winters. Long-term weather records indicate that the maximum wind gusts occur in spring; therefore wind did not affect our measures. Soil characteristics were detected in field, by visual evaluation (Mueller et al., 2009). The geotechnical parameters were determined by technical tables (Alasia et al., 2011). Soil moisture was measured by "TMS unit" (TOMST) probes, at 20-25 cm deep.

2.2. Pulling tests

An experimental test protocol defined by previous similar studies (Sani et al., 2012) was applied, with the following operating method: an inclinometer was positioned horizontally near the base of the tree, with the help of a bubble level and taking into account the pull direction. This instrument measures the tilt of root plate (resolution: hundredths of degree) related to the force of load. In the same way, an elastometer was positioned vertically at the breast height. The elastometer measures the strain (compression and tension) of the marginal fibers of the tree trunk (resolution: micron µm). A load cell (measuring range: 0-40 kN, resolution: 0.01 kN) was attached to the tree by a rope tied to the tree trunk. In the case of two main trunks, we used a pulley. The load cell was connected to the trunk at 2/3 of the plant height, thanks to the tree climbing technique. A winch applies the load (max load: 20 kN) (Fig 2.).

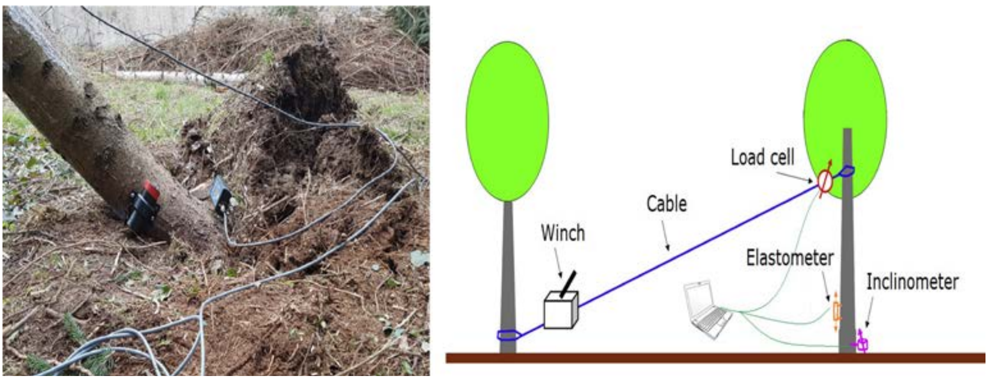

(a) **(b)**

Fig. 2. (a) Example of pulling test (Quaracchi, tree 5), (b)Pulling test scheme and measuring instruments

The test was performed by progressive and constant application of the force, developed by the 56 mm advancement of the manually operated winch cable, coupled with the continuous recording of the variation of the stress values. The used instruments were produced by Argus Electronic GMBH (TreeQinetic system). The pulling tests were carried out in two steps: in the first, to stay within the elastic field, we pulled until the tilt of root plate has reached a value of 0.20°- 0.30° of inclination - recording the force values. To subdivide the load in the vertical and horizontal component, we have measured the pull angle, related to the horizontal. This is “low load” test mode, and do not damages the tree. In the second step, we pulled up to the tree overturning. This is “high load" test mode (Wessolly, 1996). It was not possible to overturn all the plants for two main reasons: (i) the winch was not able to apply a sufficient force for bigger plants, and (ii) overturning was not always permitted for safety issues. 11 plants out of 21 have been overturned. Pulling tests are performed without taking into account the dominant wind direction.

2.3. Roots distribution and RAR measurement

In order to evaluate the root anchorage, it is necessary to know the roots distribution within the root plate. In this work, root counting by image analysis applying the trench profile wall technique photographs (Bischetti et al., 2005) was adopted. The trench was excavated manually, with dimensions varying with the tree size, while the depth was based on roots presence. Trench profile was photographed by a Nikon digital camera, at 1.6 m distance from the profile. Lens (Focal length: 24 mm) have about 80° of angle of view. This configuration permitted to take at a time a profile width of 2.6 m. Keeping this setting, it was possible to correct distortions and bind all frames of each profile. Roots were manually digitized through CAD software. *RAR* values were obtained at each depth, for increments of 10 cm, counting all visible roots. High resolution photo permitted the recognition of 0.1 mm roots diameter.

2.4. Model of root anchorage

Numerical simulations of overturning were carried out with a simple model, which calculates the SF (Factor of safety) (Eq. 2).

$$SF = \frac{\sum Ms}{\sum Mo} \qquad (2)$$

where: *Ms* is the stabilizing moment (kNm), *Mo* is the overturning moment (kNm). The stability analysis scheme is presented in Fig. 3. The overturning moment is the horizontal component of load multiplied by the pulling height (ht), while the stabilizing moment is the sum between friction and cohesion along the break area, multiplied by the root plate radius (*Rt*) (Eq. 3).

$$Ms = Rt\left[f\left(Wt + Wrp + Fv\right)\right] + \left[\left(Cv + C\right)Arp\right] \qquad (3)$$

where: *f* is the friction factor (function of the soil friction angle and of the degree of saturation), *Wt* is the tree weight(N), *Wrp* is the root plate weight (N), *Fv* is the vertical component of load of pull (N), *Cv* is the root cohesion (function of *RAR*) (kPa), *C* is the soil cohesion (kPa), *Arp* is the root plate area (m^2) (hemispherical shape, radius = *Rt*) (Fig. 3).

A parameter used to characterize the root system is αz (Eq. 4). This can be utilized to compare different plants, and it is the ratio between the radius of the root plate (*Rt*) and the radius of the plant (*DBH/2*). It corresponds to a surface distribution factor of the root system (Lobis et al., 2004; Matteck et al., 1993) (Eq. 4).

$$\alpha z = \frac{Rt}{0.5\,DBH} \qquad (4)$$

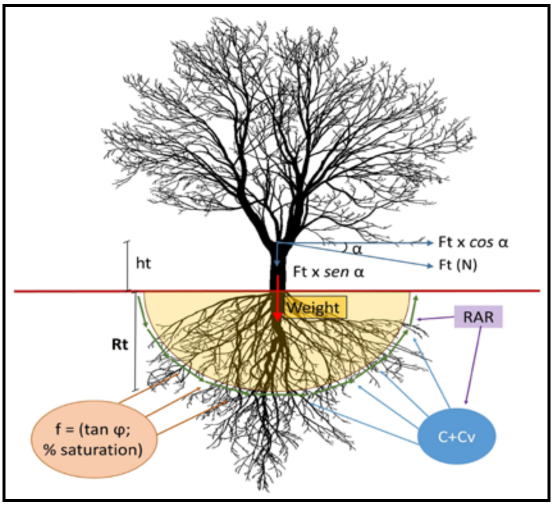

Fig. 3. Conceptual scheme of the forces

2.5 Root system shape

Usually, *RAR* is calculated on horizontal planes at increasing depths. In our case, the same methodology was applied at hemispherical surfaces, as the stabilizing friction force acts on a hemisphere given by the root system shape. Therefore, we added a reduction coefficient of 0.5, got as a form factor, by the ratio of the square area (with side "l") to the hemispherical area (with radius "l"). This coefficient can be also experimentally obtained by comparing the ratio between the *RAR* measured on a hemispherical area and the *RAR* measured on a square area, on the same root system. Arezzo's trees have very shallow root system (b<0,1 m), therefore a shape change of the modelled root soil plate was necessary, from hemispherical to cylindrical, with constant depths (measured by field analysis).

3. Results

The first interpretation of data is represented by the construction of the stress-displacement curve for each test, both for the root plate tilt and for the stem bending. The diagram shows the tree behavior: if the trunk is free from defects, the stem bending works in elastic range until the tree overturn (Fig. 4.). The stress-displacement diagrams show how the stem bending remains proportional to the applied force, which indicates that the deformation is in the elastic phase. Initially, the inclination of the root plate remains in the elastic phase, up to about 2.5°. Then, the deformation proportionally increases with load, which indicates that the deformation is in the plastic phase. The consequent root soil plate rotation causes root plate breaks. In agreement with other authors (Wessolly, 1996), at the 2.5° threshold the break of the soil-root system occurs, as the failure of the root anchorage. Beyond this threshold, increasing the applied force, the coarser roots, which are directly pulled, finally break or uproot. For the model building, the force to tilt the root plate of 2.5° is used as the force needed to overcome the root anchorage.

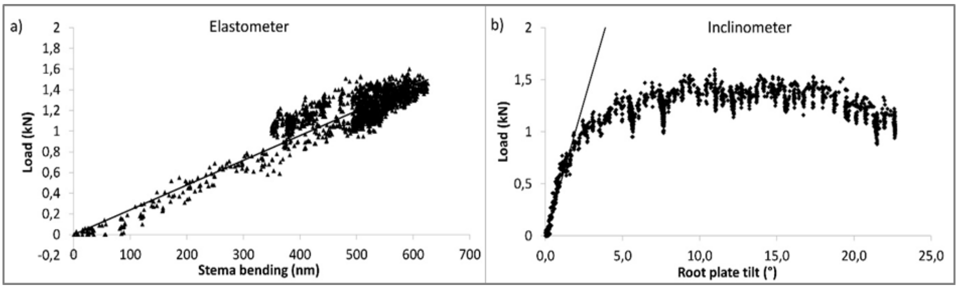

(a) (b)

Fig. 4. Stress-displacement diagrams for Inclinometer and Elastometer sensors. The straight line shows the proportionality between the two variables (example: *Alnus glutinosa*, Pomezzana)

3.1. Stress analysis

The presented results show that high and low loads are linked by a linear relationship (Fig. 6a). In fact, the analysis produced a good correlation coefficient (R^2 = 0.93) and the point cloud is well distributed around the regression line (Fig. 5a). In according with the "Generalized tipping curve" (Wessolly, 1996), the low load is equal to 23% of the high load. The maximum force ranged between the 110 and 170 % of the high load, with an average value equal to 148%. In agreement with other works (Peltola 2006, Lundström et al. 2007), a good correlation between tree size ($H*DBH^2$) and the BMmax (Fig. 5b) was found.

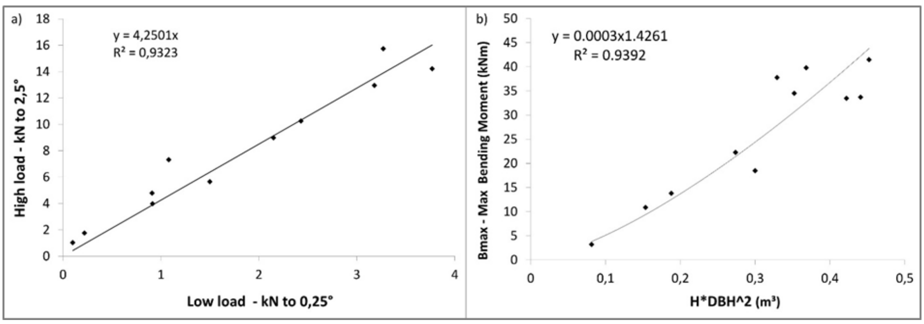

(a) (b)

Fig. 5. Correlation between High and Low load and between BMmax and tree size, for 11 overturned tree

3.2. Model applications

Measuring all the involved variables during a pulling test, and imposing *SF*=1, the model is able to return Rt. The modelled radius detects the root plate portion that withstands the wind load, in terms of weight and cohesion. We have found that this radius is bigger than the real radius verified during the pulling tests (Fig. 6). *Rt* has a fairly good correlation with both the diameter and the crown area (Fig. 7).

Rt value permits the calculation of "αz" factor (αz is the factor that links *DBH* with *Rt* (Eq. 4)). Tree stability depends on root anchorage, so we put in relation *Rt* with the mean rooting depth "*b*", factor of the *RAR* equation (Eq. (1), Fig. 8), to assess how roots distribution influences the stabilizing moment. The parameter αz varied between 4 and 12, according to the studies of Mattheck et al. (1993) and Lobis et al. (2004), and is well-linked to "*b*" ($R^2 \approx 0.9$) with a linear law.

4. Discussions

Plants support a part of wind load thanks to their crown architecture (Rudnicki et al. 2001). Branches dissipate the induced energy by a complex oscillatory behavior. This implies a changing of the crown architecture, due to the drag reconfiguration (Rodriguez et al. 2008). When wind increases, the energy is transferred more to the root system. In Fig. 5, we can see how the stem bending remains in the elastic phase, but, with the same force, root plate fails. This happens when plants are free from relevant defects of their trunk.

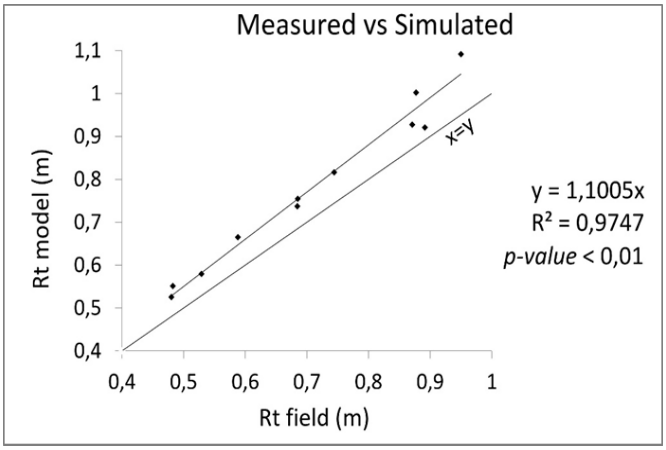

Fig. 6. *Rt* calculated by the model vs *Rt* measured in field analysis, for 11 overturned tree

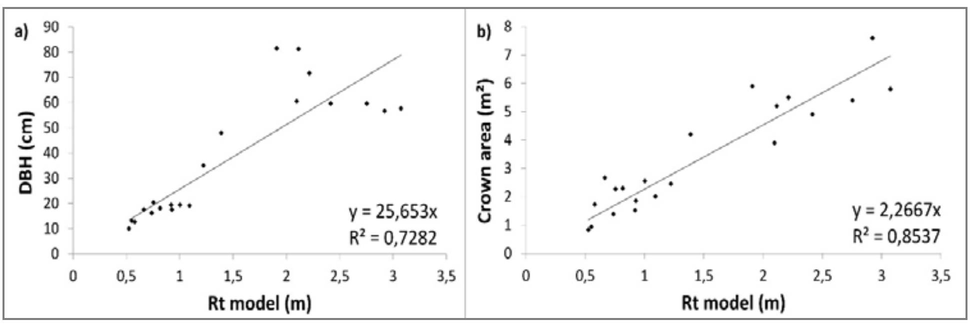

Fig. 7. Relation between *Rt* and other tree parameters

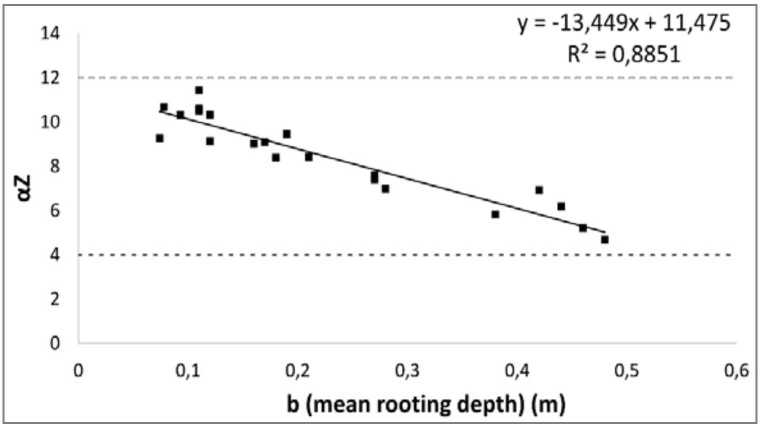

Fig. 8. Correlation between αz and the "b" factor

Each pulling test that was carried out was analyzed by the same plotting presented in Fig.5. No plan showed a different pattern. The results obtained by the inclinometer sensor show that around 2.5 ° of inclination trees have the yield strength. At this particular stress the failure of the root anchorage occurs. As argued by Wessolly (1996), the tree overturning would equally occur (within a wider time frame) by interrupting the load application, mainly due to the weight of the inclined tree. The bending moment to tilt the root plate up to 2.5° was chosen as destabilizing input in the model (neglecting the horizontal component of tree weight, when it tilts), to assess the root anchorage, precisely when it fails. If we had taken the applied max load, we would have taken into account the maximum force to uproot the tree from its rooting site (Achim, 2009). The force required to tilt the plate by 2.5° (high load), for trees subjected only to low-load testing (0.20 - 0.30°), was obtained by the law found from the comparison between the two test types (Fig.6a). The used value (Low Load = 23% High Load) is comparable with the values of the "General Tipping Curve" of Wessolly. The high variability of the max bending load (110-170% of high load) does not permit to obtain BMmax for the non-overturned trees. BMmax for the 11 overturned plants provides a clear demonstration that the performed pulling tests are coherent with other works (Peltola, 2006; Lundström et al. 2007) (Fig.6b). The link between the tree size and the maximum force to tilt the tree shows how the plant grows adapting to external and internal stresses it is subjected to. More in detail, Coutts (1983) argued that the plant adapts to the presence of dominant winds by reinforcing the root system in parallel direction to the dominant wind. This was also found in the works of Lundström (2007), who detected this fit also for plants subjected to artificial loads.

The root system influences the tree stability also according to root morphology. In the work of Fourcaud and Stokes (2008) the overturning resistance was evaluated based on the root system shape. Root distribution depends mainly on soil conditions and availability of water (Rahardjo et al., 2009; Preti et al. 2010). It also depends on genotype specific characteristics of the species. Some species are not able to develop a root system capable of providing the necessary anchorage, depending on soil conditions (Bengough et al., 2011). Even the phenological phase plays an important role in the reaction to external stress (Read et al., 2006). The root anchorage was assessed by an inverse model application. When *SF* is equal to 1, the destabilizing moment and the stabilizing moment are equivalent. To calculate the stabilizing moment it is crucial to locate the right radius of the root plate, because this determines the root plate volume, which resists the external load, thanks to friction. Furthermore, the model detects the mean rooting depth *b* used in the RAR equation. Then, the model finds *Cv*, that is the resisting cohesion between root plate and the rest of soil, against the load. *Rt* varies depending on the soil type and its characteristics and on the mean rooting depth. Moreover, it, reflects the right balance (when *SF* = 1) between weight and cohesive strength. *SF* showed a growing trend when *Rt* increases, toward *SF* = 1. However, *SF* shows a particular decreasing flexion, given that increasing *Rt* decreases *Cv*, while the weight of the plate is not sufficient for stability. Beyond *SF* = 1 the model shows that plant stability is exclusively given by weight. It is also possible to argue that the root plate breaks to a depth where there are no more roots (or very few). Determining this depth is crucial for the stability of a vegetated slope. The real *Rt*, found during the pulling tests is lower than the modelled *Rt* (Fig. 7). For the 11 plants pulled out until overturning, these two measures resulted well related to each other. The ratio between *Rt* model and *Rt* field is >1, and this shows that the root plate rotated portion (tilt 2.5 °) is greater than the one that is overturned. This is because the roots do not break (or uproot) all at the same time. In fact, when one root breaks, the root plate decreases in volume. *Rt* has a good correlation with the crown area, due to the space competition with adjacent plants. The correlation with the diameter is less good, but this is well known for the crown area too, since it also depends very much on the characteristics of the species. Finally, αz is well correlated with the "*b*" factor of the *RAR* equation. This is a further demonstration of how the plants can adapt to external agents. The root system develops within the limits imposed by the site conditions, but ensuring the best anchorage possible. The more the root system is developed in depth, the less the lateral exploration of root is needed for stability and vice versa. A similar link between rooting depth and plant stability is shown by Peltola (2006).

5. Conclusions

The developed model leads to the estimation of the root plate radius that is resistant to exterior loads. Moreover, experimental measurements demonstrated that the low-load pulling test (non-destructive and relatively inexpensive) is representative of the forces at play. Tree stability is influenced by the equilibrium between the roots distribution and the lateral space to grow. With this approach, the indirect estimation of the factor "*b*" of *RAR* equation is possible, useful for slope stability analysis. In field application, the model can also be used to design reinforcement techniques of the root anchorage, for plants with criticalities.

The model requires further verifications and a better geometric schematic adaptation to the root system type (heart, tap or plate root system). Possible future developments are: (i) comparison of the model with other indirect estimators of "b"; (ii) analysis of the movement of the root plate with ground sensors positioned around the tree, or by SfM ‘Structure-from-Motion’.

Acknowledgements

Thanks are due to the three graduate candidates Raffaele Bistondi, Marco Bellucci and Giulio Benucci, who contributed to field work. GESAAF's staff (Enrico Guastini, Paolo Trucchi, Marco Togni, Lucia Castellucci) is thanked for the analysis support and for the authorization procedures.

References

Achim A., Nicoll B.C., (2009), Modelling the anchorage of shallow-rooted trees, *Forestry*, **82**, 273-284.

Alasia U., Pugno M., (2011), Construction Course 5 - Earth Mechanics (in Italian: Corso di Costruzioni 5 - Meccanica delle Terre), *SEI*, 400, On line at:

http://libria1jg.tk/8805070688/corso-di-costruzioni-con-espansione-online-per-gli-ist-tecnici-5-di-umberto-alasia-maurizio-pugno.pdf

Chiaradia E.A., Simonato T., Speziali B., Vitali B., Vullo P., Zocco A., (2005), Root strength and root area ratio of forest species in Lombardy (Northern Italy), *Plant and Soil*, **278**, 11-22.

Coutts M.P., (1983), Root architecture and tree stability, *Plant and Soil*, **71**, 171-188.

Coutts M.P., Grace, J., (1995), *Wind and Trees*, Cambridge University Press New York, USA.

Dani F., Laio F., (2010), Root profile assessment by means of hydrological, pedological and above-ground vegetation information for bio-engineering purposes, *Ecological Engineering*, **36,** 305-316.

Danjon F., Fourcaud T., Bert D., (2005), Root architecture and wind-firmness of mature *Pinus pinaster*, *New Phytologist*, **168**, 387-400.

De Langre M.E., Moulia B., (2008), A scaling law for the effects of architecture and allometry on tree vibration modes suggests a biological tuning to modal compartmentalization. *American Journal of Botany*, **95**, 1523-1537.

Dupuy L., Fourcaud T., Stokes A., (2005), A numerical investigation into the influence of soil type and root architecture on tree anchorage, *Plant and Soil*, **278**, 119-134.

Ewers M.L., Telewski F.W., (2000), Thigmomorphogenesis: changes in the morphology and mechanical properties of two Populus hybrids in response to mechanical perturbation, *Tree Physiology*, **20**, 535-540.

Fourcaud T., Ji J.N., Zhang Z.Q., Stokes A., (2008), Understanding the impact of root morphology on overturning mechanisms: A modelling approach, *Annals of Botany*, **101**, 1267-1280.

Gardiner B.A. (1994). Wind and wind forces in a plantation spruce forest, *Boundary-Layer Meteorology*, **67**, 161-186.

Greenwood J.R., (2006), SLIP4EX - A program for routine slope stability analysis to include the effects of vegetation, reinforcement and hydrological changes, *Geotechnical and Geological Engineering*, **24**, 449-465.

James K., Hallam C., Spencer C., (2013), Measuring tilt of tree structural root zones under static and wind loading, *Agricultural and Forest Meteorology*, **168**, 160-167.

James K.R., Kane B., (2008), Precision digital instruments to measure dynamic wind loads on trees during storms, *Agricultural and Forest Meteorology*, **148**, 1055-1061.

Kay L.B.D., Hu C., Li Y., Schindler U., Behrendt A., Ball, B.C., (2009), Visual assessment of soil structure: Evaluation of methodologies on sites in Canada, China and Germany, Part I., *Soil & Tillage Research*, **103**, 179-187.

Kellomäki H.S., Hassinen A., Granander M., (2000), Mechanical stability of Scots pine, Norway spruce and birch: An analysis of tree-pulling experiments in Finland, *Forest Ecology and Management*, **135**, 143-153.

Lobis V., Ambrosi P., Maresi G., Salvadori C., La Porta N., (2004), At the root of the problem (in Italian: Alla radice del problema), *Acer*, **6**, 29-34

Lundström T., Jonas T., Stöckli V., Ammann W., (2007), Anchorage of mature conifers: resistive turning moment, root-soil plate geometry and root growth orientation, *Tree Physiology*, **27**, 1217-1227.

Mattheck C., Bethge K., (2000), Simple mathematical approaches to tree biomechanics, *Arboricultural Journal*, **24**, 307-326.

Mattheck C., Bethge K., Erb D., (1993), Failure criteria for trees, *Arboricultural Journal*, **17**, 201–209.

Mattheck C., Teschner M., Schäfer J., (1997), Mechanical control of root growth: A computer simulation, *Journal of Theoretical Biology*, **184**, 261-269.

Mckenzie A.G.B.M., Hallett P.D., Valentine T.A., (2011), Root elongation, water stress, and mechanical impedance: A review of limiting stresses and beneficial root tip traits, *Journal of Experimental Botany*, **62**, 59-68.

Meredieu V.C., Stokes A., De Coligny F., Suarez J., Gardiner B.A., (2005), Modelling the windthrow risk for simulated forest stands of Maritime pine (*Pinus pinaster* Ait.), *Forest Ecology and Management*, **213**, 184-196.

Mickovski S.B., Bengough G., Bransby M.F., Davies M.C.R., Hallett P.D., Sonnenberg R., (2007), Material stiffness, branching pattern and soil matric potential affect the pullout resistance of model root systems, *European Journal of Soil Science*, **58**, 1471-1481.

Moore J.R., (2000), Differences in maximum resistive bending moments of *Pinus radiata* trees grown on a range of soil types, *Forest Ecology and Management*, **135**, 63-71.

Moulia B., Coutand C., Julien J.-L., (2015), Mechanosensitive control of plant growth: bearing the load, sensing, transducing, and responding, *Frontiers in Plant Science*, doi: 10.3389/fpls.2015.00052.

Peltola H.M., (2006), Mechanical stability of trees under static loads, *American Journal of Botany*, **93**, 1501-1511.

Penman J., Gytarsky M., Hiraishi T., Krug T., Kruger D., Wagner F., (2003), Good practice guidance for land use, land use change and forestry, IPCC National Greenhouse Gas Inventories Programme and Institute for Global Environmental Strategies, Kanagawa, Japan. On line at: http://www.ipccnggip.iges.or.jp/public/gpglulucf/gpglulucf.htm .

Rahardjo H., Harnas F.R., Indrawan I.G.B., Leong E.C., Tan P.Y., Fong Y.K., Ow L.F., (2014), Understanding the stability of Samanea saman trees through tree pulling, analytical calculations and numerical models, *Urban Forestry and Urban Greening*, **13**, 355-364.

Read J., Stokes A., (2006), Biomechanics in an ecological context, *American Journal of Botany*, **93**, 1546-1565.

Rudnicki M., Silins U., Lieffers V.J., Josi G., (2001), Measure of simultaneous tree sways and estimation of crown interactions among a group of trees, *Trees - Structure and Function*, **15**, 83-90.

Sani L., Lisci R., Moschi M., Sarri D., Rimediotti M., Vieri M., Tofanelli S., (2012), Preliminary experiments and verification of controlled pulling tests for tree stability assessments in Mediterranean urban areas, *Biosystems Engineering*, **112**, 218-226.

Schelhaas M.J., Kramer K., Peltola H., van der Werf D.C., Wijdeven S.M.J., (2007), Introducing tree interactions in wind damage simulation, *Ecological Modelling*, **207**, 197-209.

Schindler D., (2008), Responses of Scots pine trees to dynamic wind loading, *Agricultural and Forest Meteorology*, **148**, 1733-1742.

Tabacchi G., Di Cosmo L., Gasparini P.M.S., (2011), Estimation of the volume and the phytomass of the main Italian forest species. Forecast equations, volume tables and tables of the epigeal arboreal plant, (In italian: Stima del volume e della fitomassa delle principali specie forestali italiane. Equazioni di previsione, tavole del volume e tavole della fitomassa arborea epigea), Consiglio per la ricerca e la sperimentazione, Unità di ricerca per il monitoraggio e la pianificazione forestale, Trento, Italy.

Tardìo G., Gonzàlez-Ollauri A., Mickovski S.B., (2016), A non-invasive preferential root distribution analysis methodology from a slope stability approach, *Ecological Engineering*, **97**, 46-57.

Telewski F.W., (2006), A unified hypothesis of mechanoperception in plants, *American Journal of Botany*, **93**, 1466-1476.

Wessolly L., (1996), Stability of trees, explanation of the tipping process, *Stadt Und Grün*, **4**, 268-272.